Supplementary Figure 1. Statistical analysis of engraftment levels in recipient mice.

a, Statistical analysis (one-way ANOVA followed by Tukey post-hoc test; ns, not significant) of the data presented in Fig. 1a (percentage of hCD45$^+$ cells in the blood of recipient mice). **b**, Numbers of recipient mice that reach an engraftment level of at least 10% hCD45$^+$ cells in the blood 7-9 weeks after transplantation. **c**, Blood engraftment levels of the mice used in Fig. 1c for analysis of the BM. **d**, Statistical analysis, similar to (**a**), of the data presented in Fig. 1c (percentage of hCD45$^+$ cells in the BM of recipient mice). **e**, Absolute numbers of hCD45$^+$ cells in the BM (2 femurs and 2 tibias) of recipient mice shown in Fig. 1c. The lower number of cells in the BM of MISTRG is due to the smaller size of the mice at that age (10-12 weeks post-transplantation), likely due to reduced human-to-mouse phagocytic tolerance.

a

	Rag2$^{-/-}$ *Il2rg*$^{-/-}$	NSG	MITRG	MISTRG
n	56	142	155	105
Mean	2.9	31.4	24.0	35.8
SEM	0.5	1.7	1.8	2.7

One-way ANOVA : $p < 0.0001$

Tukey	*Rag2*$^{-/-}$ *Il2rg*$^{-/-}$	NSG	MITRG	MISTRG
Rag2$^{-/-}$ *Il2rg*$^{-/-}$				
NSG	p<0.05			
MITRG	p<0.05	p<0.05		
MISTRG	p<0.05	ns	p<0.05	

b

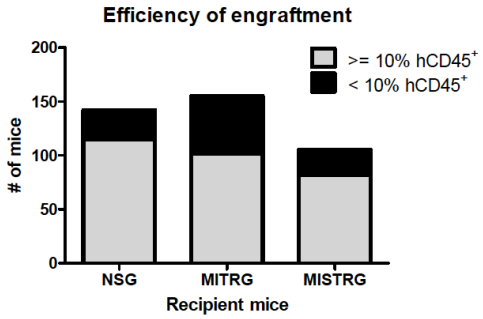

c

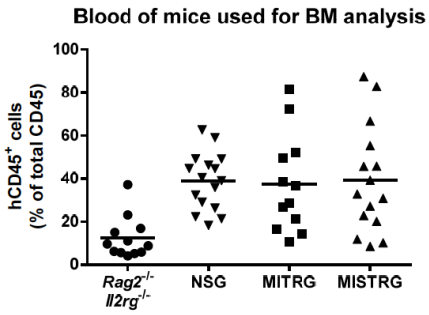

d

	Rag2$^{-/-}$ *Il2rg*$^{-/-}$	NSG	MITRG	MISTRG
n	12	16	12	15
Mean	47.7	81.0	93.7	89.0
SEM	8.8	2.6	1.4	3.0
Min	4.2	59.6	84.1	61.8
Max	96.1	96.1	99.7	98.9

One-way ANOVA : $p = 0.0042$

Tukey	NSG	MITRG	MISTRG
NSG			
MITRG	p<0.05		
MISTRG	ns	ns	

e

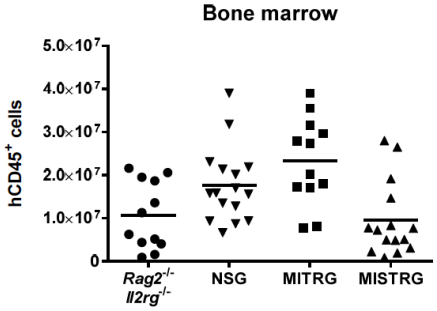

Supplementary Figure 2. Engraftment of MISTRG mice with adult CD34$^+$ cells.

a, Irradiated MISTRG mice were transplanted with 100,000 CD34$^+$ cells isolated from human fetal liver, cord blood or adult peripheral blood after G-CSF mobilization. Engraftment levels (% hCD45+ cells) in the blood of recipient mice was measured 4-5 and 7-8 weeks later (n=11-13 mice/group, using at least 2 human donors for each group). **b-c**, Representative flow cytometry analysis (**b**) and quantification (**c**) of engraftment levels in the blood and BM of MISTRG mice 22 weeks after transplantation with adult, G-CSF-mobilized CD34+ cells (n=3).

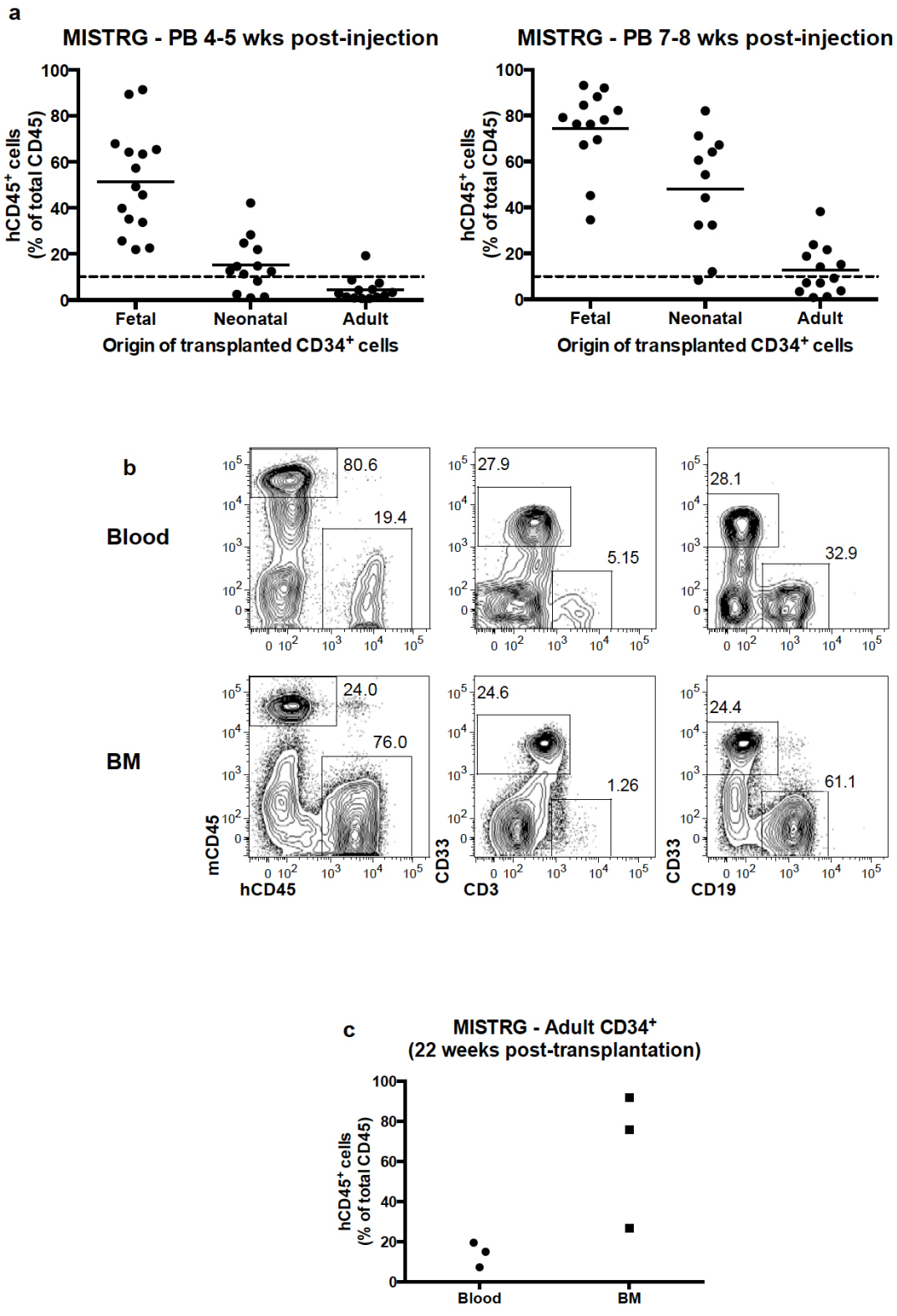

Supplementary Figure 3. Enhanced human myeloid development in MI(S)TRG mice.

a, Statistical analysis (one-way ANOVA followed by Tukey post-hoc test; ns, not significant) of the data presented in Fig. 2a (percentage of hCD33$^+$ cells in the blood of recipient mice). **b-c**, Frequencies (**b**) and statistical analysis (**c**) of human myeloid cells (hCD33$^+$) in the BM of recipient mice. **d**, Representative flow cytometry analysis of human lymphoid and myeloid lineages in the blood of MISTRG. **e**, Human WBC composition in MISTRG mice engrafted without prior irradiation, as described in Fig. 1d,e (n=8; error bars indicate SEM). **f-g**, Absolute numbers of human myeloid cells (hCD33$^+$) in the lung (**f**) and liver (**g**) of recipient mice (n=8-12; p-values calculated by one-way ANOVA followed by Tukey posthoc test, * p<0.05).

a

	Rag2$^{-/-}$ *Il2rg*$^{-/-}$	NSG	MITRG	MISTRG
n	20	122	129	88
Mean	3.5	8.5	29.8	40.9
SEM	0.4	0.5	1.5	1.9

One-way ANOVA : p < 0.0001

Tukey	*Rag2*$^{-/-}$ *Il2rg*$^{-/-}$	NSG	MITRG	MISTRG
Rag2$^{-/-}$*Il2rg*$^{-/-}$				
NSG	ns			
MITRG	p<0.05	p<0.05		
MISTRG	p<0.05	p<0.05	p<0.05	

b

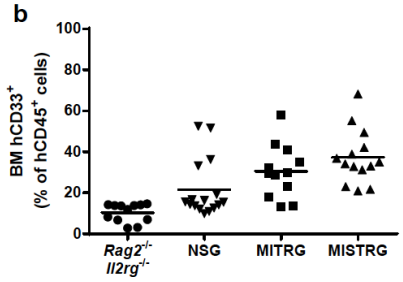

c

	Rag2$^{-/-}$ *Il2rg*$^{-/-}$	NSG	MITRG	MISTRG
n	12	16	12	14
Mean	10.3	21.6	30.5	37.3
SEM	1.3	3.5	3.8	3.5

One-way ANOVA : p < 0.0001

Tukey	*Rag2*$^{-/-}$ *Il2rg*$^{-/-}$	NSG	MITRG	MISTRG
Rag2$^{-/-}$*Il2rg*$^{-/-}$				
NSG	ns			
MITRG	p<0.05	ns		
MISTRG	p<0.05	p<0.05	p<0.05	

d

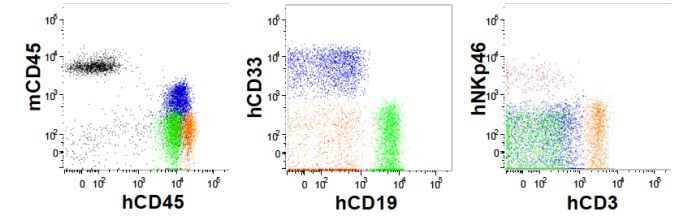

e

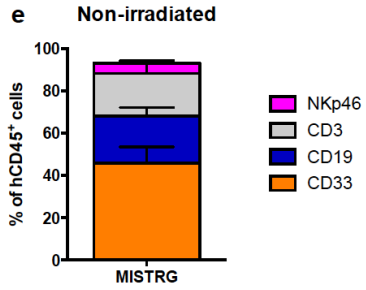

f

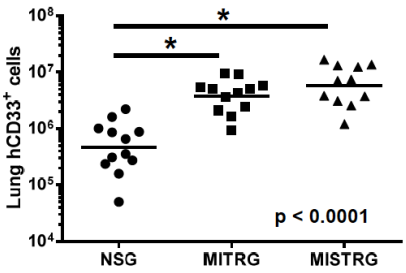

g

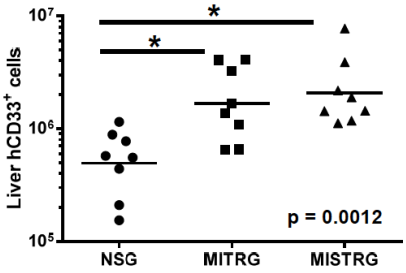

Supplementary Figure 4. Human neutrophils, eosinophils, and basophils are present in MISTRG mice.

a-b, Representative flow cytometry analysis (**a**) of human monocytes (blue, $CD33^{hi}SSC^{lo}CD66^{-}$) and neutrophils (green, $CD33^{+}SSC^{hi}CD66^{+}$), and quantification (**b**) of neutrophils in the BM of recipient mice. **c**, Representative flow cytometry analysis of the same human cell populations in the blood of MISTRG and human healthy donor. **d-e**, Representative flow cytometry analysis (**d**) and quantification (**e**) of human eosinophils in BM and blood of NSG and MISTRG mice. Human eosinophils were gated as $hCD45^{+}$Lineage $(Lin)^{-}SSC^{hi}$Siglec-8^{+} cells. Lineage makers used were hCD3, hCD19, hCD14, and hCD56. **f-g**, Representative flow cytometry analysis (**f**) and quantification (**f**) of human basophils in BM and blood of NSG and MISTRG mice. Human basophils were gated as $hCD45^{+}$Lineage $(Lin)^{-}$FceRIa^{+} cells. p-values were calculated by Student's *t*-test. Results are representative of or combined from two experiments.

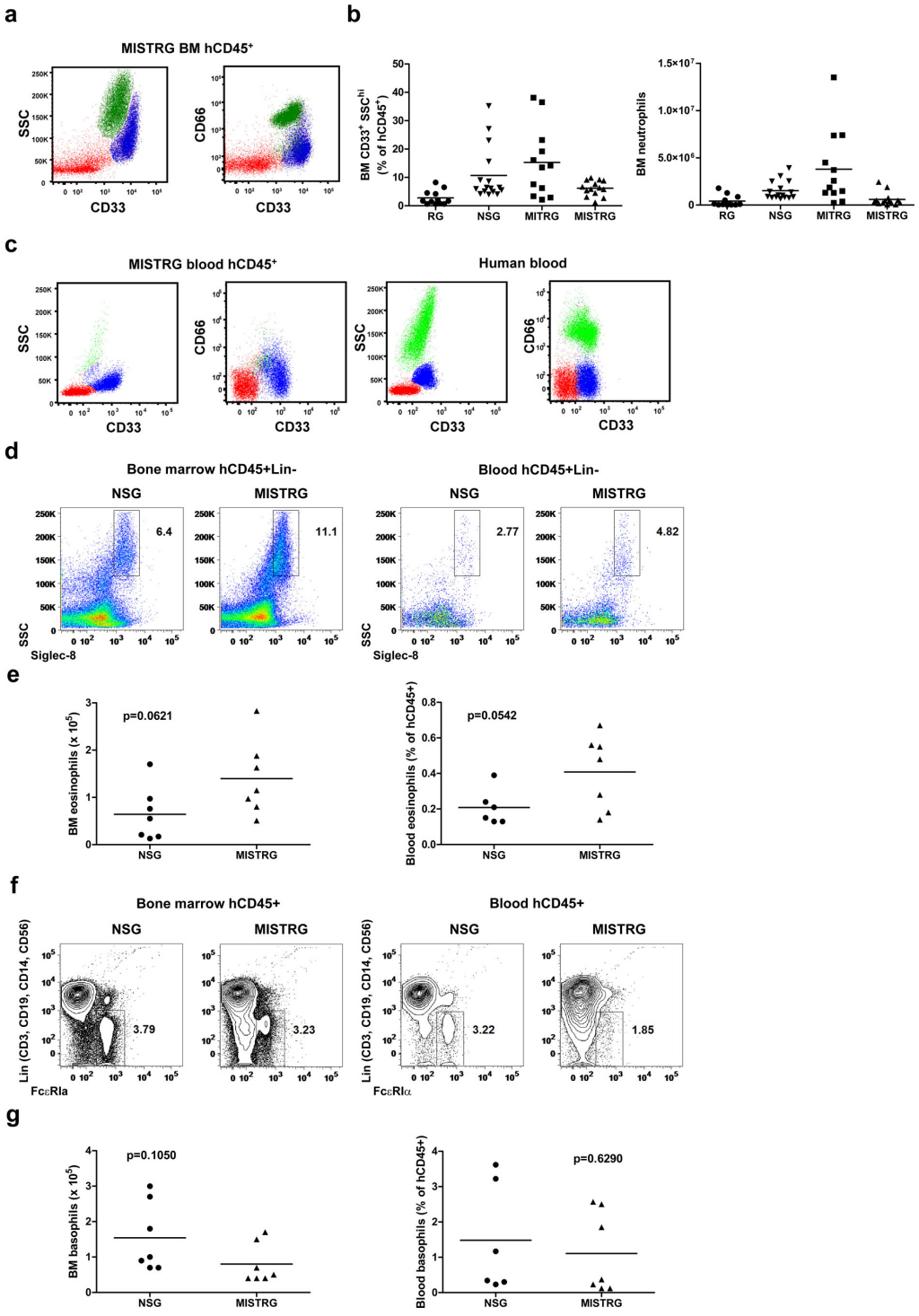

Supplementary Figure 5. Phenotypic and functional characterization of human dendritic cells.

a-c, Representative flow cytometry analysis (a) and quantification of human conventional (**b**) and plasmacytoid (**c**) dendritic cells in the bone marrow and spleen of NSG and MISTRG mice (n = 7 mice/group, data combined from 2 independent experiments). **d**, Representative flow cytometry analysis of $CD1c^+$ (BDCA-1) and $CD141^+$ (BDCA-3) subsets of conventional dendritic cells in MISTRG. **e**, Expression of co-stimulatory molecules (CD80 and CD86) by human dendritic cells 6h after injection of PBS (blue) or LPS (red) in MISTRG. The numbers indicate mean MFI of 3 independent mice from 1 experiment.

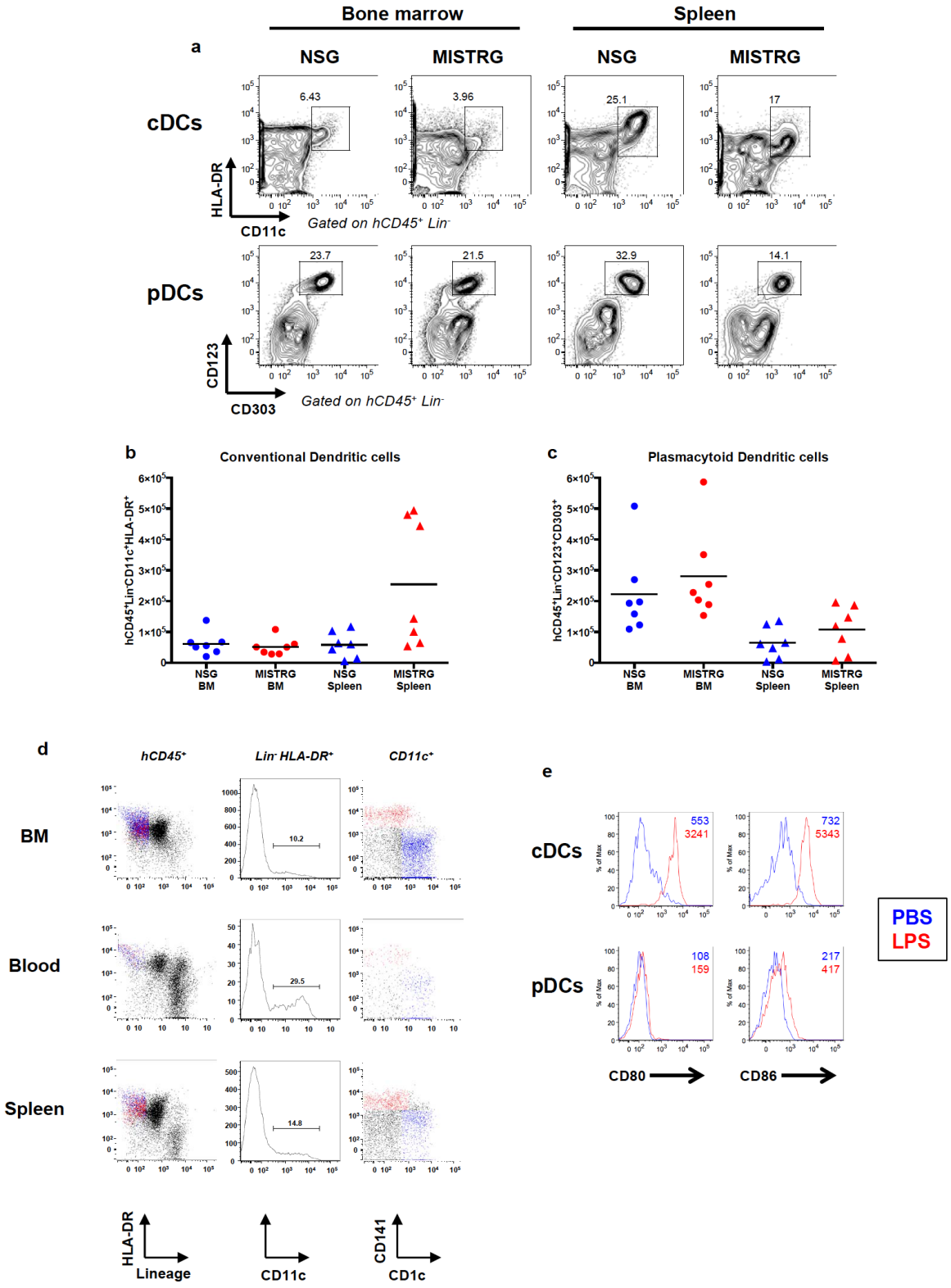

Supplementary Figure 6. Enhanced development of human monocyte subsets in MI(S)TRG mice.

a, Representative flow cytometry analysis of human monocyte subsets, identified by expression of CD14 and CD16 among hCD45^{+}CD33^{+} cells in the BM, spleen, lung and liver of the indicated recipient mice. **b**, Frequencies (error bars represent SEM) among hCD33^{+} cells and absolute numbers of monocyte subsets in the lung and liver of recipient mice (n=12 mice/group; p-values calculated by one-way ANOVA; *, p<0.05 Tukey post hoc test).

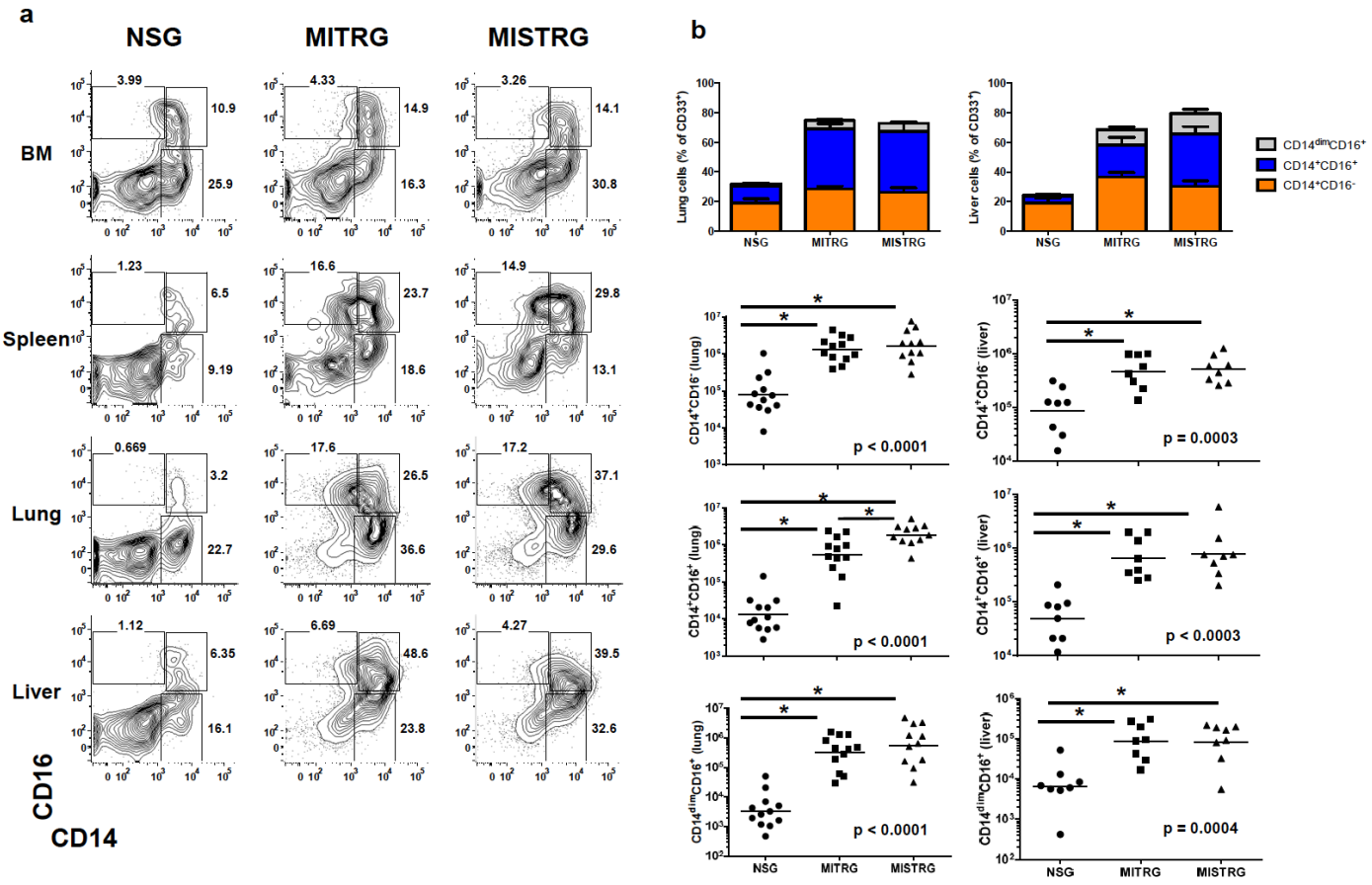

<u>Supplementary Figure 7</u>. Human monocyte subsets are similar in MISTRG and in human donors.

Extended immunophenotype of the indicated subsets of human monocytes in the BM of MISTRG recipients and human donor. Staining with isotype control antibodies is shown in red and specific antibodies in blue.

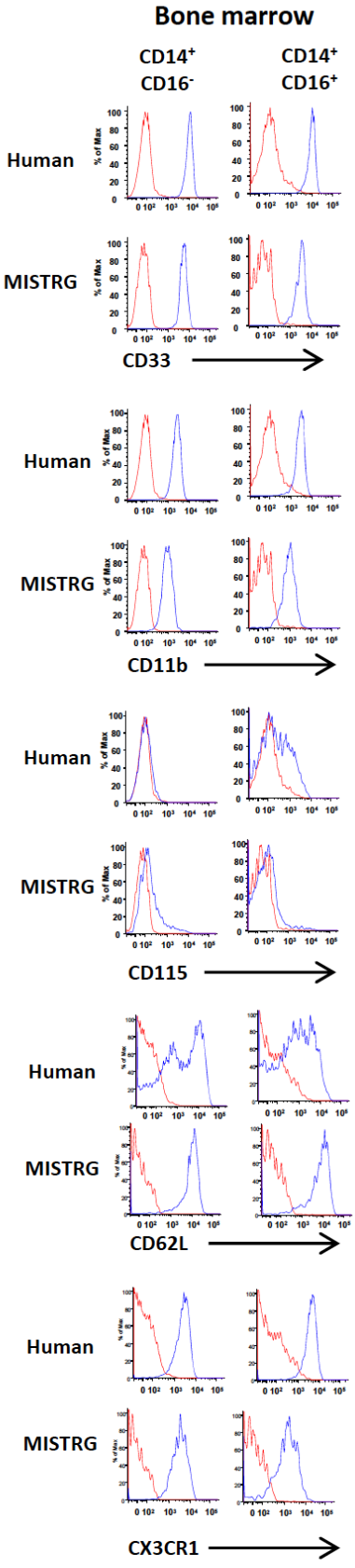

Supplementary Figure 8. MISTRG mice provide human IL-15/IL-15Ra.

a, Quantitative RT-PCR analysis of human IL-15 and IL-15Ra mRNA expression in the lung of engrafted NSG, MITRG, and MISTRG mice (n=7-8; p-values calculated by one-way ANOVA; *, p<0.05 Tukey post hoc test). Expression was normalized to mouse *Hprt*. **b**, Flow cytometry analysis of IL-15Ra expression on human cell populations ($hCD45^{+}mCD45^{-}$) from blood of engrafted MISTRG mice (representative of n=4). Blue and red histograms represent staining with isotype control or with IL-15Ra antibody, respectively. Results are representative of or combined from two experiments.

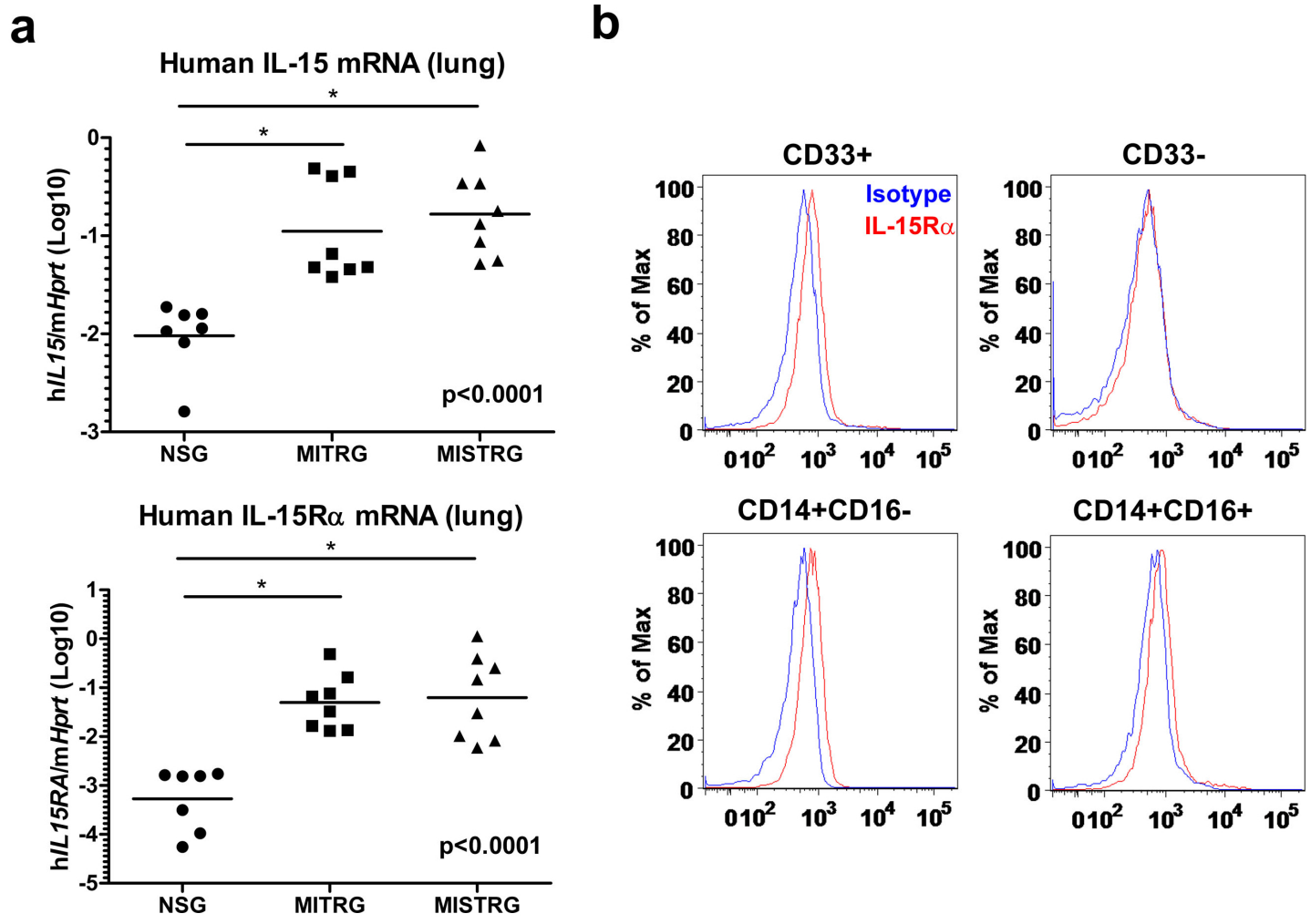

Supplementary Figure 9. Enhanced human NK cell development in MISTRG mice.

a-b, Frequency (**a**) and absolute number (**b**) of human NK cells (hNKp46^{+} hCD3^{-}) in engrafted NSG, MITRG, and MISTRG mice (n=8-16; p-values calculated by one-way ANOVA; *, p<0.05 Tukey post hoc test). Results are combined from four experiments.

a

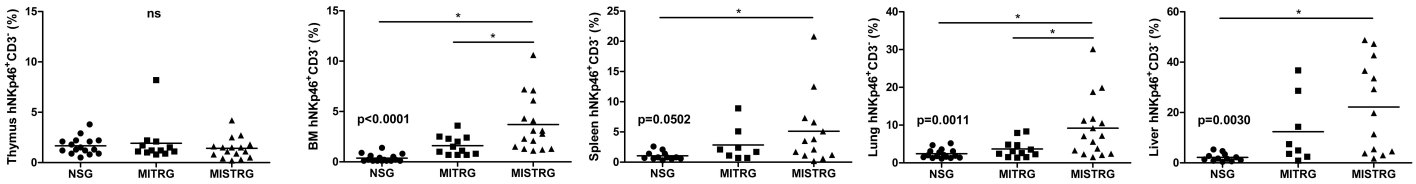

b

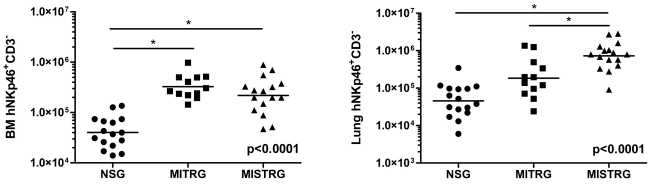

<u>Supplementary Figure 10</u>. Bona fide human NK cells, showing enhanced maturation, are present in MISTRG mice.

a, Flow cytometry analysis of CD94 and CD161 expression on human blood NK cells from a human donor and engrafted MISTRG (n=3). Blue and red histograms represent staining with isotype control Abs or with CD94/CD161 Abs, respectively. **b**, Flow cytometry analysis of KIR expression on human blood NK cells from a human donor or from engrafted MISTRG mice (n=3). Numbers indicate frequencies of KIR^+ cells. **c-d**, CD16 surface expression on human NK cells from engrafted NSG, MITRG, and MISTRG mice (n=4-8; p-values calculated by one-way ANOVA; *, p<0.05 Tukey post hoc test). Results are representative of or combined from one (**a, b**) or four (**c, d**) experiments.

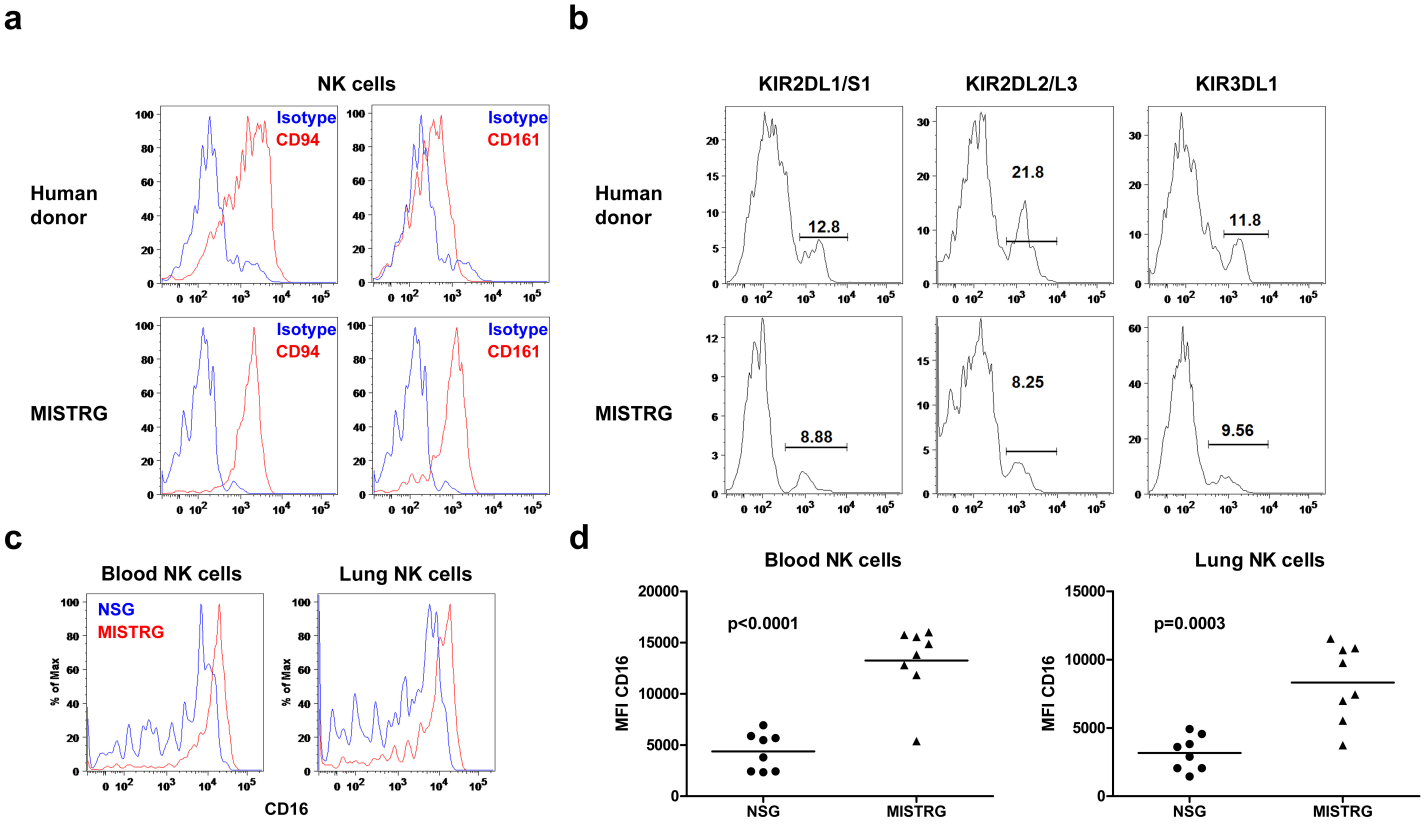

Supplementary Figure 11. Characterization of human B cell phenotype and function.

a, Quantification of the percentage of human B cells ($CD19^+$ cells) among $hCD45^+$ cells in the blood of RG, NSG, MITRG and MISTRG mice (n=20-113 mice/group; the same data was used in Fig. 2b). **b-c**, Representative flow cytometry analysis (**b**) and quantification (**c**) of the expression of maturation markers by human B cells in the bone marrow, spleen and blood of NSG and MISTRG mice (n=7 mice/group, combined from 2 independent experiments). **d**, Mice were immunized with Ovalbumin (2 immunizations with CFA and IFA, respectively). The presence of Ovalbumin-specific human IgM in the serum prior to immunization (pre-immune) or 10 days after the second immunization was measured by ELISA (n=8-11 mice/group). The dashed horizontal line represents mean + 2 S.D. of pre-immune serum.

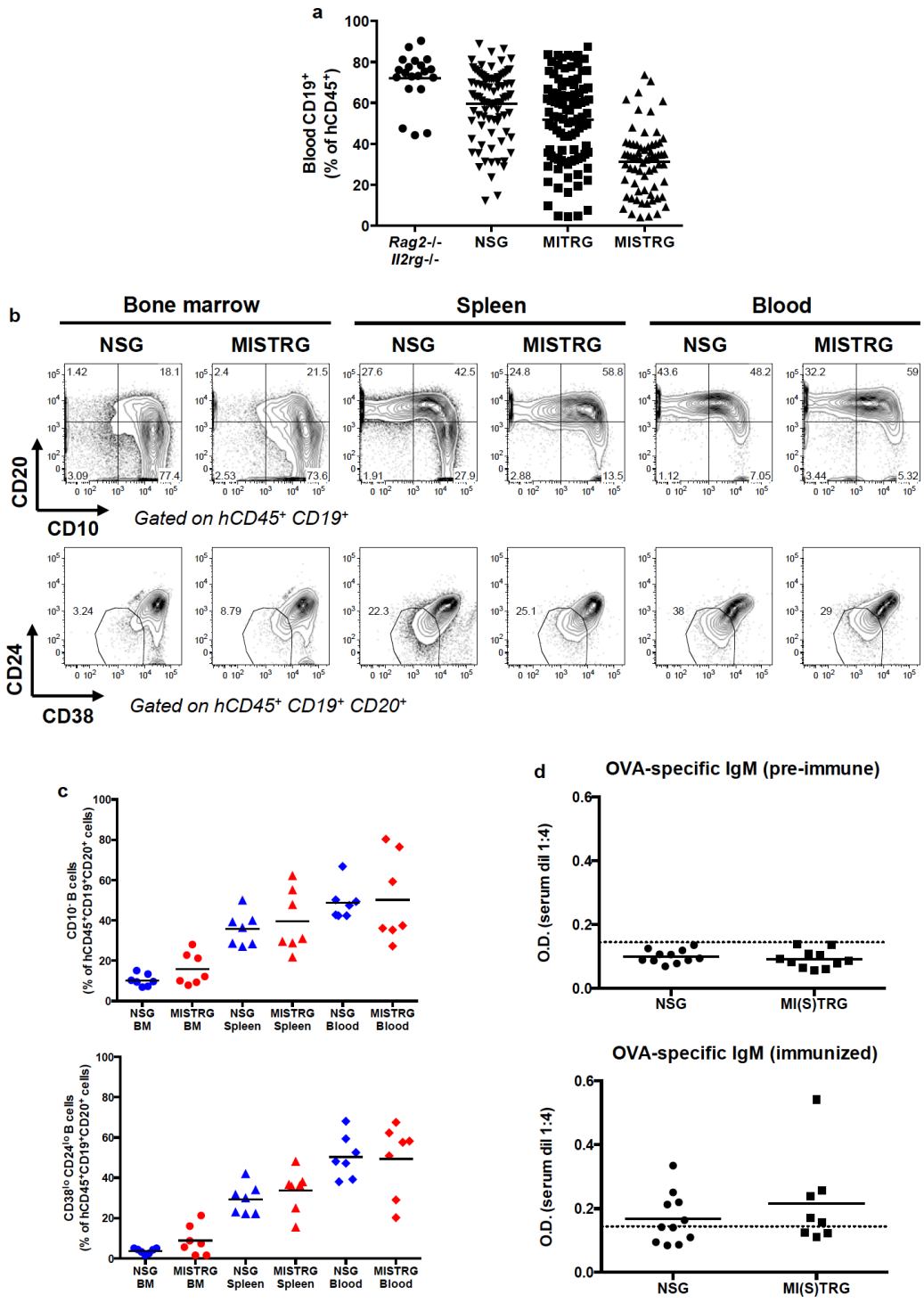

Supplementary Figure 12. Functional human T cells develop in MISTRG mice.

a, Quantification of the percentage of human T cells ($CD3^+$ cells) among $hCD45^+$ cells in the blood of RG, NSG, MITRG and MISTRG mice (n=20-113 mice/group; the same data was used in Fig. 2b). **b**, Representative flow cytometry analysis of human blood T cells ($CD3^+$) from NSG and MISTRG mice. **c**, Phenotype of human CD4 and CD8 T cells in the blood of NSG and MISTRG mice. **d-e**, Frequency (**d**) and representative flow cytometry analysis (**e**) of IFNg-expressing human liver T cells from either uninfected or Listeria-infected NSG and MISTRG mice (n=5-15; p-value calculated by one-way ANOVA). Results are representative of or combined from two experiments.

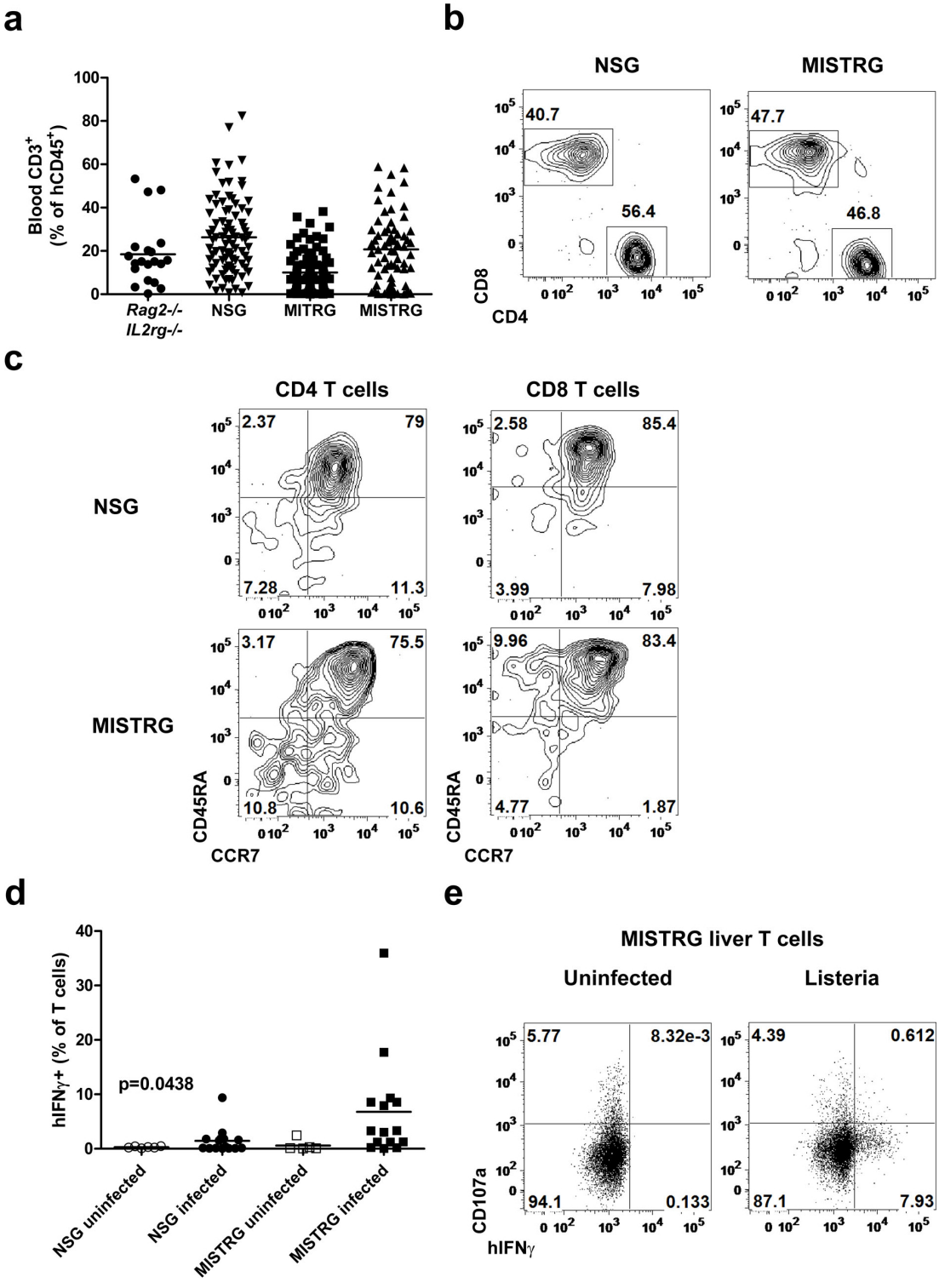

Supplementary Figure 13. Immunohistochemistry of human myeloid cells infiltrating melanoma.

Representative immunohistochemistry staining of human myeloid cells in tumors from NSG, MISTRG or human patients. Three subject per group, and 3 pictures per subject are shown.

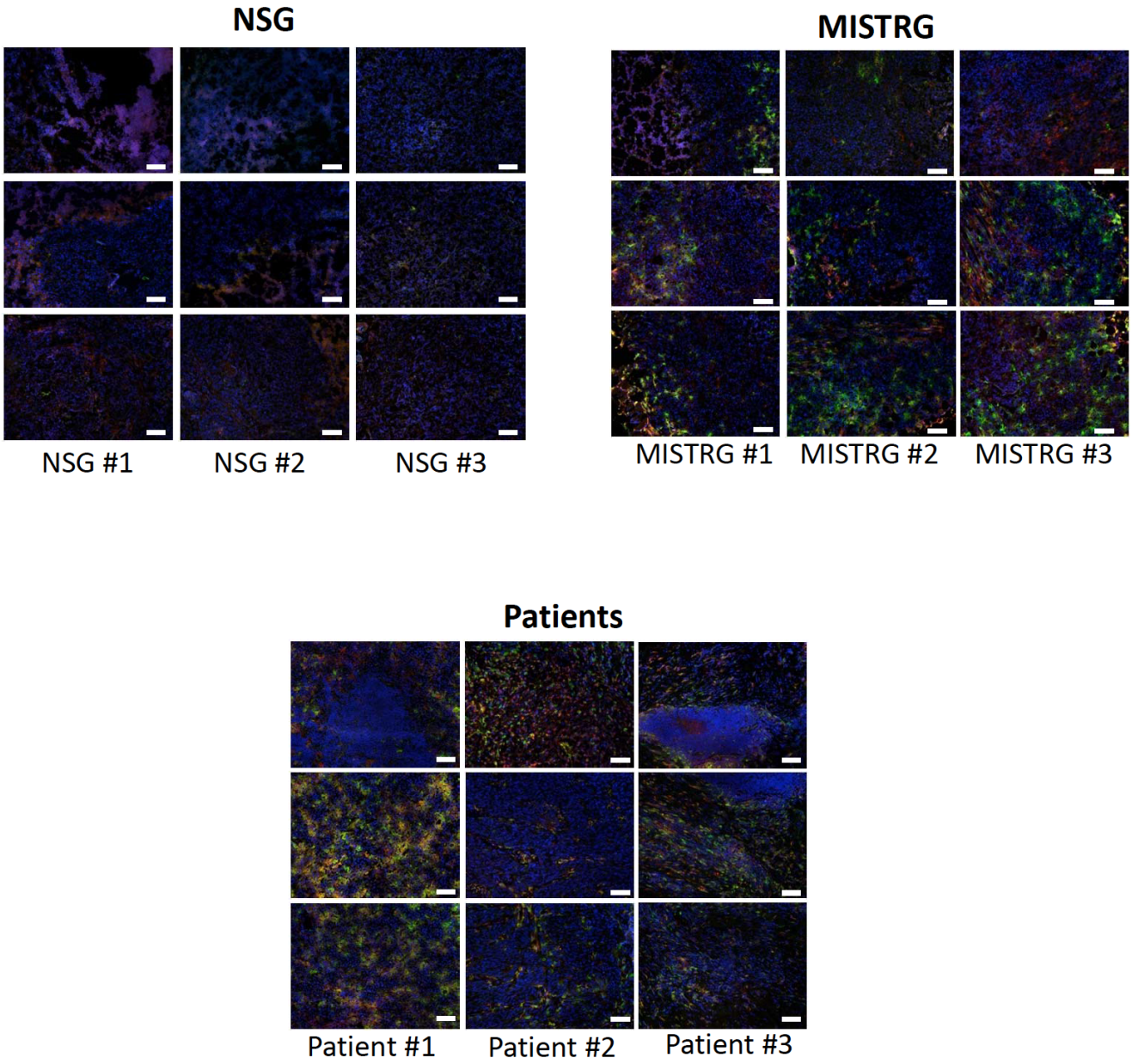

Supplementary Table 1

Engraftment levels and immune cell development and function in various recipient mice

	Rag2$^{-/-}$ *Il2rg*$^{-/-}$	*Rag2*$^{-/-}$ *Il2rg*$^{-/-}$ TPO$^{h/h}$	*Rag2*$^{-/-}$ *Il2rg*$^{-/-}$ IL-3/GM-CSF$^{h/h}$	*Rag2*$^{-/-}$ *Il2rg*$^{-/-}$ M-CSF$^{h/h}$	hSIRPα^{tg} *Rag2*$^{-/-}$ *Il2rg*$^{-/-}$ *or* NSG	MISTRG	Human
Blood hCD45^{+} (%)	5-20	5-20	5-20	20-40	10-60	10-80	100
BM hCD45^{+} (%)	20-80	75-90	20-80	20-80	60-90	85-99	100
Human CD33^{+} myeloid cells (% of hCD45^{+})	1-7	10-20	5-10	10-30	5-15	30-50	50-70
Human NK cells (% of hCD45^{+})	0-1	ND	ND	ND	0.5-2	1-7	1-6
Human NK cell function	Immature	ND	ND	ND	Immature	Functional	Functional
Serum TNFα (ng/ml, 90 min post-LPS)	ND	ND	ND	ND	0.3-3	10-200	ND
Lung alveolar macrophages	Absent	Absent	Present	Absent	Absent	Present	Present

ND: Not determined
Rag2$^{-/-}$ *Il2rg*$^{-/-}$ TPO$^{h/h}$: Ref 16
Rag2$^{-/-}$ *Il2rg*$^{-/-}$ IL-3/GM-CSF$^{h/h}$: Ref 17
Rag2$^{-/-}$ *Il2rg*$^{-/-}$ M-CSF$^{h/h}$: Ref 18
hSIRPα^{tg} *Rag2*$^{-/-}$ *Il2rg*$^{-/-}$: Ref 28